



Review

# High-Entropy Materials for Lithium Batteries

Timothy G. Ritter<sup>1</sup> , Samhita Pappu<sup>2</sup> and Reza Shahbazian-Yassar<sup>2,\*</sup> 

<sup>1</sup> Department of Civil & Materials Engineering, University of Illinois Chicago, Chicago, IL 60607, USA; tritter2@uic.edu

<sup>2</sup> Department of Mechanical & Industrial Engineering, University of Illinois Chicago, Chicago, IL 60607, USA; spappu3@uic.edu

\* Correspondence: rsyassar@uic.edu

† Lead contact.

**Abstract:** High-entropy materials (HEMs) constitute a revolutionary class of materials that have garnered significant attention in the field of materials science, exhibiting extraordinary properties in the realm of energy storage. These equimolar multielemental compounds have demonstrated increased charge capacities, enhanced ionic conductivities, and a prolonged cycle life, attributed to their structural stability. In the anode, transitioning from the traditional graphite (372 mAh g<sup>-1</sup>) to an HEM anode can increase capacity and enhance cycling stability. For cathodes, lithium iron phosphate (LFP) and nickel manganese cobalt (NMC) can be replaced with new cathodes made from HEMs, leading to greater energy storage. HEMs play a significant role in electrolytes, where they can be utilized as solid electrolytes, such as in ceramics and polymers, or as new high-entropy liquid electrolytes, resulting in longer cycling life, higher ionic conductivities, and stability over wide temperature ranges. The incorporation of HEMs in metal–air batteries offers methods to mitigate the formation of unwanted byproducts, such as Zn(OH)<sub>4</sub> and Li<sub>2</sub>CO<sub>3</sub>, when used with atmospheric air, resulting in improved cycling life and electrochemical stability. This review examines the basic characteristics of HEMs, with a focus on the various applications of HEMs for use as different components in lithium-ion batteries. The electrochemical performance of these materials is examined, highlighting improvements such as specific capacity, stability, and a longer cycle life. The utilization of HEMs in new anodes, cathodes, separators, and electrolytes offers a promising path towards future energy storage solutions with higher energy densities, improved safety, and a longer cycling life.



**Citation:** Ritter, T.G.; Pappu, S.; Shahbazian-Yassar, R. High-Entropy Materials for Lithium Batteries.

*Batteries* **2024**, *10*, 96. <https://doi.org/10.3390/batteries10030096>

Academic Editors: Leon L. Shaw, Carlos Ziebert and Maziar Ashuri

Received: 8 February 2024

Revised: 29 February 2024

Accepted: 4 March 2024

Published: 8 March 2024



**Copyright:** © 2024 by the authors. Licensee MDPI, Basel, Switzerland. This article is an open access article distributed under the terms and conditions of the Creative Commons Attribution (CC BY) license (<https://creativecommons.org/licenses/by/4.0/>).

**Keywords:** high-entropy materials; lithium-ion batteries; anodes; cathodes; electrolytes; lithium–sulfur; metal–air

## 1. Introduction

In recent years, the development and improvement of battery technologies have become paramount, as they underpin the evolution of various industries, ranging from consumer electronics to electric vehicles and renewable energy storage. Lithium-ion batteries (LIBs) have stood as the cornerstone of rechargeable energy storage systems for several years, with the specific energy of a commercial battery pack increasing from 80 Wh kg<sup>-1</sup> in 1991 to over 360 Wh kg<sup>-1</sup> in 2023 [1]. The success of LIBs is largely attributed to their high energy density, reliability, and versatile applicability. However, as the electrification of all sectors of the economy continues, there is an increasing need for advanced battery materials that can push the boundaries and provide higher energy storage beyond the current yearly incremental growth. In view of this, recent trends have seen increased research in the area of high-entropy materials (HEMs). HEMs are a relatively new class of materials with a unique set of properties that cover a wide range of applications such as high-strength materials, corrosion resistance, catalysis, energy storage, and biomedical applications. These materials are multielement compounds with an equimolar composition that form stable single solid solutions [2]. In energy storage applications, HEMs have shown promise in

anodes, electrolytes, cathodes, and catalysis due to their high capacities, from multi-metal ions, enhanced ionic conductivities, and their high structural stability leading to increased cycle life. Therefore, the present review starts by covering the main concepts and properties of high-entropy materials, along with a discussion of how these materials are generally characterized. The main focus is on the current state of battery components, such as anodes, cathodes, electrolytes, separators, and catalysts, and how HEMs can be used to improve the performance of these components. It is observed that previous reviews have focused on energy storage across a broad array of applications, such as catalysis, hydrogen storage, supercapacitors, oxygen evolution reactions, and rechargeable batteries [3,4]. Nevertheless, a focused review of the implications of using HEMs in various components of batteries has not been discussed before. The inclusion of HEMs in new battery components is beneficial due to their enhanced capacities and higher stabilities, which can lead to improved charge storage and cycle life of batteries. In the anode, graphite has long served as the workhorse due to its high stability. Nevertheless, graphite's limited theoretical capacity has propelled research into alternative materials with higher energy storage capabilities. High-entropy anodes benefit from their improved structural stability, which reduces the material stress during charge/discharge and thereby extends the cycle life of the battery. Simultaneously, the storage capacity is also extended far beyond the limits of a graphite anode. Several cathode chemistries have evolved over the years, such as lithium iron phosphate (LFP), nickel manganese cobalt oxide (NMC), and lithium cobalt oxide (LCO), and are commonly used in LIBs. New advances in high-entropy synthesis have led to the potential of high-entropy materials replacing these cathode compositions due to their enhanced structural stabilities leading to an improvement in the cycle life and energy density. Additionally, incorporating multiple elements in the cathode composition reduces the percentage of expensive elements, such as cobalt and nickel, thus enabling the creation of cost-effective cathodes. The critical elements, which generally have increased costs, can be substituted with more cost-effective alternatives. High-entropy materials, combined with polymers or as standalone ceramic materials, can also be used as new electrolytes with applications beyond LIBs such as in sodium ion batteries or lithium–sulfur batteries. These electrolytes aim at increasing the ionic conductivity while maintaining the electrode/electrolyte interface for use in new solid-state batteries. The world of energy storage is at the precipice of transformation, driven by innovations in anode materials, cathode chemistries, and solid electrolytes. Incorporating HEMs into future battery components will decrease the overall cost per unit of energy (USD/mAh) through increased capacities and other performance enhancements. With the recent development of cost-effective synthesis methods, such as ball milling, microwave, electrochemical, aerosol, and co-precipitation methods, scalable synthesis methods have emerged, which can be adapted to industrial levels of output. The summary below aims to identify some of the recent advances and provide possible future research paths.

## 2. Basics of High-Entropy Materials

### 2.1. Background and Basic Equations

Throughout recorded history, individuals have melded metals to enhance various physical attributes in them like strength, durability, ductility, conductivity, and luster. The exploration of alloys can be traced back to ancient times, approximately 2500 BCE, when the fusion of copper and tin gave rise to the creation of bronze. Noteworthy alloys such as bronze, brass, and steel share a common characteristic—they are comprised of a predominant element (copper for bronze and brass, iron for steel) that is blended with trace amounts of other elements like tin in bronze or carbon in steel. The modest proportions of additional elements in most alloys are emblematic of conventional alloying practices and are typically controlled during the synthesis process. Traditionally, during alloying, the added elements substitute an atom of the predominant element at the lattice position. Many contemporary alloys consist of a primary element, with supplementary elements incorporated at lower concentrations. For example, in the case of 6061 aluminums, Al

constitutes 98.56%, with Mg and Si as the next highest concentrations. High-entropy alloys (HEAs), in contrast, exhibit a near-equi-molar composition, comprising five or more elements, with no single element dominating the composition. This positions the composition toward the center of the phase diagram, departing from the conventional placement at the periphery that is seen for traditional alloys. The absence of any one element as the majority in the composition stands out as a key distinction between traditional alloy systems and high-entropy materials (HEMs).

An alternative method for discerning between traditional and high-entropy systems lies in their crystal structure. In traditional alloys' unit cell, the predominant element is typically encircled by either similar predominant elements or by single atoms of elements that are present in lower concentrations. Conversely, a high-entropy unit cell with an equimolar composition of five elements in the crystal structure will likely have its closest neighboring atoms be dissimilar atoms. This results from the random and equal distribution of all atoms throughout the structure. The arrangement of atoms in a traditional alloy and an HEM alloy can be seen below in Figure 1. In Figure 1A, the majority atom (gray balls) makes up a large percentage of the composition and is surrounded by small quantities of other elements (differently colored balls). In Figure 1B, there is no element that makes up the majority of the composition, and all atoms are randomly distributed in the structure. The stochastic arrangement of atoms significantly boosts entropy in HEAs, contributing to the creation of distinctive material properties.

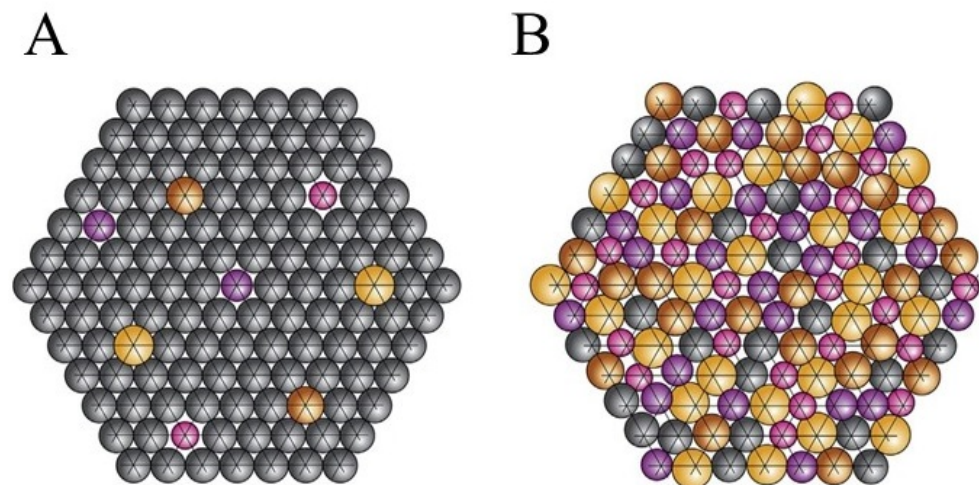


**Figure 1.** Schematic of unit cells. (A) Traditional unit cell. (B) HEM unit cell. Reprinted with permission from ref. [5]. Copyright© 2017 Elsevier (Amsterdam, The Netherlands).

Further, the formation of phase diagrams and crystal structures is influenced by the thermodynamic conditions in a system, as determined by two primary equations: the Gibbs free energy (Equation (1)) and the Boltzmann entropy equation (Equation (2)) [2]. The Gibbs free energy ( $\Delta G_{mix}$ ) consolidates the enthalpy ( $\Delta H_{mix}$ ), temperature (T), and entropy ( $\Delta S_{mix}$ ) into a single parameter, serving as a key indicator for predicting spontaneous reactions and the formation of stable solutions. A reaction is likely to occur spontaneously when the Gibbs free energy is negative, achieved through negative enthalpy (typical for traditional materials) or a sufficiently large entropy term that drives the total Gibbs energy below zero [2]. The Boltzmann equation establishes a connection between the system entropy and the potential microstates. In materials with high entropy, the increases are attributed to the random alignment of atoms. Equation (2) illustrates the configurational entropy for both cation and anion positions, with R presenting the gas constant, S1 being cation sites, S2 being anion sites, and  $X_i$  and  $X_j$  representing the molar composition of each element [2]. In conventional alloys with a dominant element and several minor elements, the system's entropy remains low. Conversely, in the creation of HEMs with equimolar compositions, the entropy term can be maximized, facilitating the formation of stable solid solutions.

$$\Delta G_{mix} = \Delta H_{mix} - T\Delta S_{mix} \quad (1)$$

$$S_{config} = -R \left[ \left( \sum_{i=1}^N X_i \ln X_i \right)_{S1} + \left( \sum_{j=1}^M X_j \ln X_j \right)_{S2} \right] \quad (2)$$

In the case of an equimolar composition, the Boltzmann equation is simplified to Equation (3), where  $R$  represents the gas constant and  $N$  is the count of equimolar elements [2]. Defining a specific threshold for high entropy can vary slightly, but is generally considered to be achieved when the entropy attains a minimum value of  $1.5R$ , necessitating the presence of five or more equimolar elements.

$$S_{config} = R [\ln N] \quad (3)$$

The determination of whether a material will attain a state of high entropy is governed by the system's thermodynamics, as influenced by the Gibbs free energy and the Boltzmann equation. Traditional alloying techniques often fall short in meeting this criterion for high entropy. Consequently, novel synthesis techniques must be developed to enable the attainment of this elevated level of mixing.

## 2.2. Four Core Effects

High-entropy materials are characterized and defined by four key concepts: the high-entropy effect, lattice distortion effect, sluggish diffusion effect, and the cocktail effect [2,5–7]. These fundamental factors collectively contribute to shaping the distinctive features of HEMs. Figure 2 highlights the four core effects that are attributed to high-entropy materials.

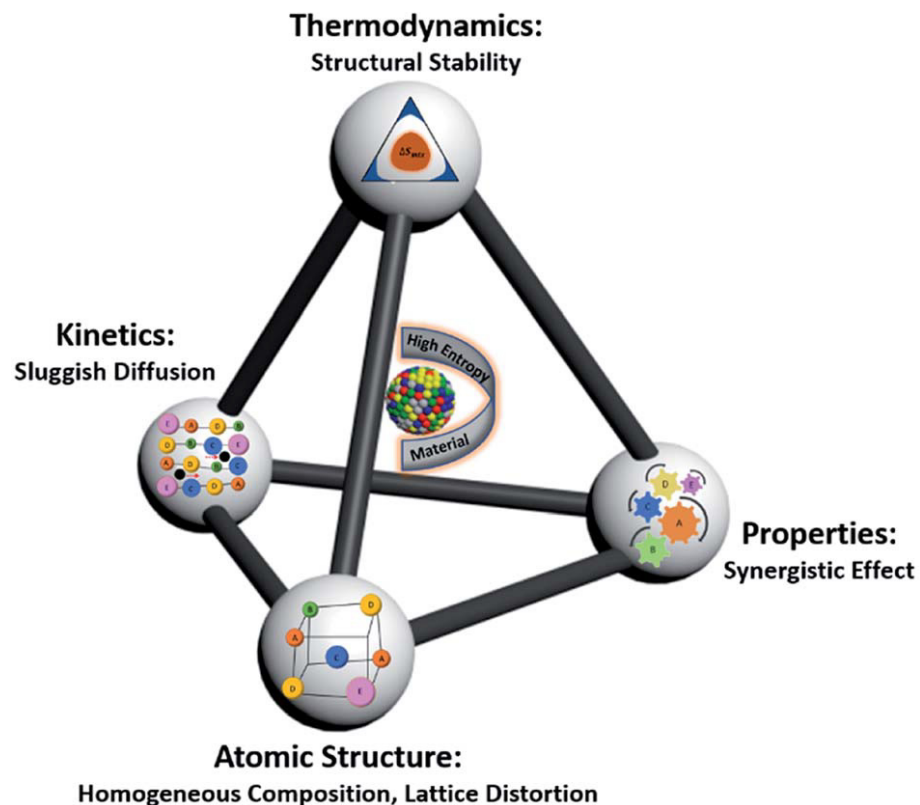


**Figure 2.** Schematic of four core effects in high-entropy materials. Reprinted with permission from ref. [2]. Copyright© 2020 Royal Society of Chemistry (London, UK).

The primary characteristic and foundational aspect of HEMs is the high-entropy effect. The elevation in entropy is a consequence of the heightened configurational entropy within the system, as previously mentioned. While various types of entropy exist, such as vibrational, electronic, and magnetic, it is the configurational entropy that takes precedence, exerting a dominating influence [5]. This rise in configurational entropy surpasses the enthalpy term in the Gibbs free energy equation (refer to Equation (1)), leading to a reduction in the free energy of the structure and consequently enhancing the system's stability for HEM formation [2]. The augmented configurational entropy facilitates the creation of stable solid solutions [6].

The second phenomenon is the lattice distortion effect, stemming from the disparate sizes of atoms within the crystal structure [2,5]. In a typical alloy's crystal arrangement, the introduction of minor atoms induces local strains, resulting in a subtle lattice distortions. In the case of HEMs, a notable degree of strain is evident in the crystal lattice due to the diverse sizes of each element that is distributed randomly throughout the structure. These lattice distortions contribute to a reduced intensity in the X-ray diffraction peaks and can be associated with the lower thermal conductivities observed in HEMs due to increased scattering. Additionally, this heightened strain can contribute to the reinforcement and fortification of HEMs [6].

The third impact is characterized by a delayed diffusion process, arising from the lattice distortions that impeded the motion of atoms within the structure [2]. Each atom within the crystal lattice finds itself encircled by diverse neighboring elements. The central atom, positioned at a specific site, experiences substantial interaction with the surrounding atoms, leading to varied bonding energies between them [7]. Consequently, this variance in bonding energies contributes to an elevation in activation energies within the HEMs, heightening the challenge of facilitating substitutional diffusion.

The phenomenon known as the cocktail effect characterizes the distinctive attributes of HEMs. In conventional alloys, supplementary elements are often introduced to enhance properties, such as corrosion resistance or hardness, typically interacting solely with the primary element. In contrast, the incorporation of additional elements in HEMs results in interactions not only with a primary element but also with multiple neighboring elements. This heightened level of interaction, stemming from the extensive mixing in the structure, gives rise to HEM properties that surpass the cumulative qualities of their individual components. The blending of multiple elements yields unforeseen properties that a single element alone cannot provide [8]. The interplay among diverse elements introduces an element of unpredictability, resulting in HEMs possessing distinctive physical properties.

The specific properties that are found in HEMs are contingent upon the synthesis process employed. Varied synthesis techniques yield different HEMs, including high-entropy alloys, oxides, carbides, etc., each exhibiting diverse characteristics such as strength, conductivity, and thermal and magnetic properties. The development towards high-entropy materials, as depicted in Figure 3, has spanned many years and has been propelled by an overall increase in chemical complexity. The complexity has increased as new elements represented the majority element and additional elements were included in minor concentrations in the compositions, increasing the overall entropy of the system.



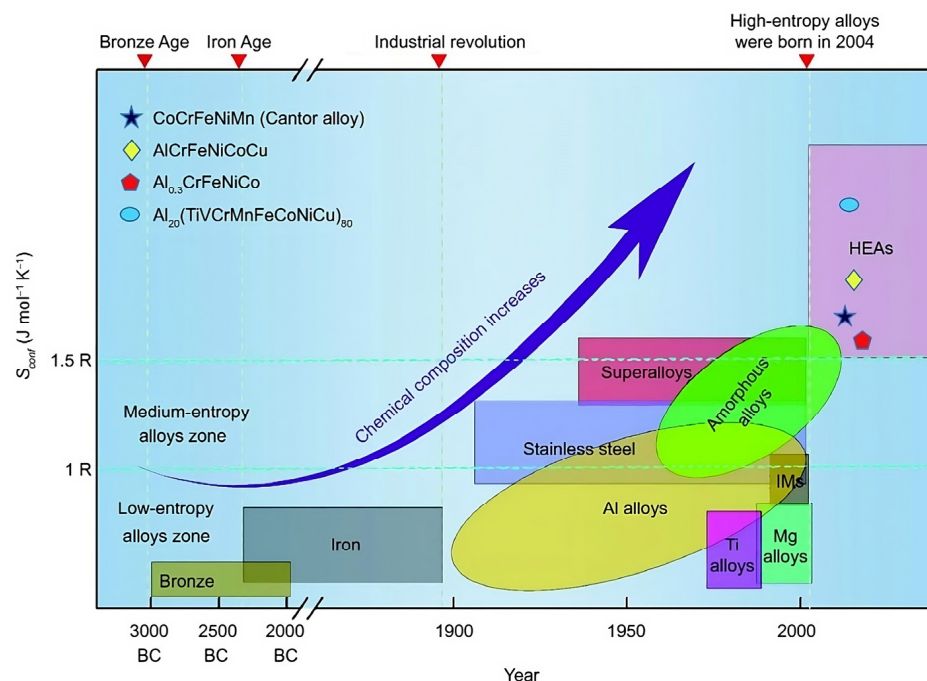


**Figure 3.** History of the development of high-entropy materials. Reprinted with permission from ref. [9]. Copyright© 2018 Springer Nature (Berlin, Germany).

### 2.3. Characterization of High-Entropy Materials

Several methods are available to determine whether a high-entropy material has been successfully produced. Phase identification can be achieved through either X-ray diffraction (XRD) or selected area electron diffraction (SAED). Many HEMs that are formed through common HEM synthesis techniques exhibit simple crystal structures, such as rock salt, FCC, BCC, Cubic, and spinel structures. These structures can easily be identified by XRD and SAED patterns [10–12]. Basic crystal structures become apparent when a single-phase solution is formed, distinguishing it from a material with different phases, which is not a characteristic of an HEM [4]. However, relying solely on XRD and SAED is insufficient for confirming the successful synthesis of an HEM.

Microscopy techniques, such as scanning electron microscopy (SEM) and transmission electron microscopy (TEM), along with high-resolution TEM (HR-TEM) when nanoparticles are involved, are necessary to study the morphology of a material. In conjunction with the microscopy, energy-dispersive X-ray spectroscopy (EDX) is used to quantify the homogenous distribution of elements within a particle [4,13]. A well-formed HEM particle should exhibit homogeneous distribution of all elements at the atomic scale, which can be observed with EDX mapping techniques.

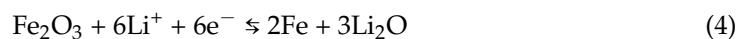
Some elemental compositions, like those involving lithium, are not easily studied using EDX techniques. The use of lithium in HEMs is common, especially in battery applications. The most precise method for determining material composition is through the use of inductively coupled plasma–optical emission spectroscopy (ICP-OES). This method helps to acquire the exact distribution of elements in the material. When lithium is included in a high-entropy material, performing ICP-OES becomes necessary, as many synthesis techniques involve elevated temperatures, and there is a concern that temperatures exceeding 800 °C during the synthesis can result in lithium evaporation [4].

## 3. Components of High-Entropy Batteries

### 3.1. Anodes

Graphite has been used as a common anode material in Li-ion batteries for several years. Its intercalation mechanism makes it very stable, but it suffers from a low theoretical capacity of 372 mAh g<sup>−1</sup> [4]. Transition metal oxides (TMOs) have been widely studied as

active materials for new LIBs, offering large theoretical capacities compared to conventional graphite anodes [2]. Materials such as  $\text{Co}_x\text{O}_y$ ,  $\text{ZnO}$ ,  $\text{CuO}$ ,  $\text{Mn}_x\text{O}_y$ ,  $\text{Fe}_3\text{O}_4$ , and  $\text{Fe}_2\text{O}_3$  are attracting attention due to their high capacity and low price [14]. For instance, iron oxides are attractive candidates for anodes due to their natural abundance, non-toxicity, and low cost. For example,  $\text{Fe}_2\text{O}_3$  has the following reaction mechanism and exhibits a theoretical specific capacity of  $1006 \text{ mAh g}^{-1}$  [15]:



Cobalt oxides, such as  $\text{CoO}$  and  $\text{Co}_3\text{O}_4$ , have attracted attention due to their advanced redox properties [15]. For instance,  $\text{CoO}$  has a theoretical specific capacity of  $716 \text{ mAh g}^{-1}$ , as indicated by the following reaction:



Manganese oxides, such as  $\text{MnO}$  and  $\text{Mn}_2\text{O}_3$ , are abundant on the Earth; have a low potential (1.03 and 1.43 V), low polarization, and high theoretical capacity ( $756$  and  $1018 \text{ mAh g}^{-1}$ ); and are environmentally friendly [15]. Other TMOs, such as  $\text{NiO}$  and  $\text{CuO}$ , have also been studied for potential anode applications. A summary of the theoretical capacities of these TMOs can be found in Table 1.

**Table 1.** Summary of the characteristics of various transition metal oxides for lithium-ion batteries [16].

Material	Voltage (V)	Specific Capacity ( $\text{mAh g}^{-1}$ )	Gravimetric Energy Density ( $\text{Wh kg}^{-1}$ )
MnO	1.03	756	779
FeO	1.61	746	1201
CoO	1.80	715	1287
NiO	1.95	718	1400
CuO	2.25	674	1517
$\text{Mn}_2\text{O}_3$	1.43	1018	1455
$\text{Fe}_2\text{O}_3$	1.63	1007	1641
$\text{Cr}_2\text{O}_3$	1.09	1058	1153

Although these TMOs have higher theoretical specific capacities, their crystal structures undergo significant volume changes during cycling, leading to rapid capacity decay [2,15]. This limitation restricts their applications for long-term stable and efficient batteries.

Recently, entropy-stabilized metal oxides have been suggested as a replacement for graphite anodes due to their excellent Li-ion conductivity and stabilized crystal structures [2]. A recent study on  $(\text{Co}_{0.2}\text{Cu}_{0.2}\text{Mg}_{0.2}\text{Ni}_{0.2}\text{Zn}_{0.2})\text{O}$  with a rock salt structure demonstrated an initial discharge capacity of  $980 \text{ mAh g}^{-1}$  [14]. The composition of this material can be modified to create a medium-entropy oxide (MEO) anode by selectively removing individual elements from the structure. It was observed that removing a single element affected the electrochemical behavior and long-term cycling of the entire material [17]. This improvement in cycle stability was attributed to the increased structural stability of the HEM. The structure remains highly stable with cycling, as Cu and Co are electrochemically active and participate in the conversion reaction, while others such as Mg contribute to maintaining the structural integrity [2]. Ni and Zn are also used to increase the energy density of the material, while Zn benefits from a low lithiation/delithiation potential, delivering a high output voltage and energy density [18,19]. Guo et al. showed that modifications to high-entropy oxides can result in a long cycling life (1000 cycles) while maintaining a high capacity of  $460 \text{ mAh g}^{-1}$  at charging rates of  $1000 \text{ mA g}^{-1}$  [20]. At lower charging rates of  $100 \text{ mA g}^{-1}$ , the capacity exceeds  $950 \text{ mAh g}^{-1}$  after 200 cycles, proving the high structural stability of high-entropy materials when used as anodes [20]. Lökçü et al. highlighted that the inclusion of lithium into a high-entropy rock salt structure

resulted in the creation of a greater number of oxygen vacancies within the structure [21]. This increase in oxygen vacancies led to a higher discharge capacity, reaching a maximum of  $1930 \text{ mAh g}^{-1}$  at 35% Li inclusion [21]. Table 2 below shows a summary of a select number of high-entropy anodes and their cycling characteristics. Figure 4 illustrates the cycle life of several such high-entropy anodes. The various anodes are a combination of elements from Table 1 and highlight their increased capacities over traditional graphite anodes while maintaining the capacity for a large number of cycles at high charging rates.

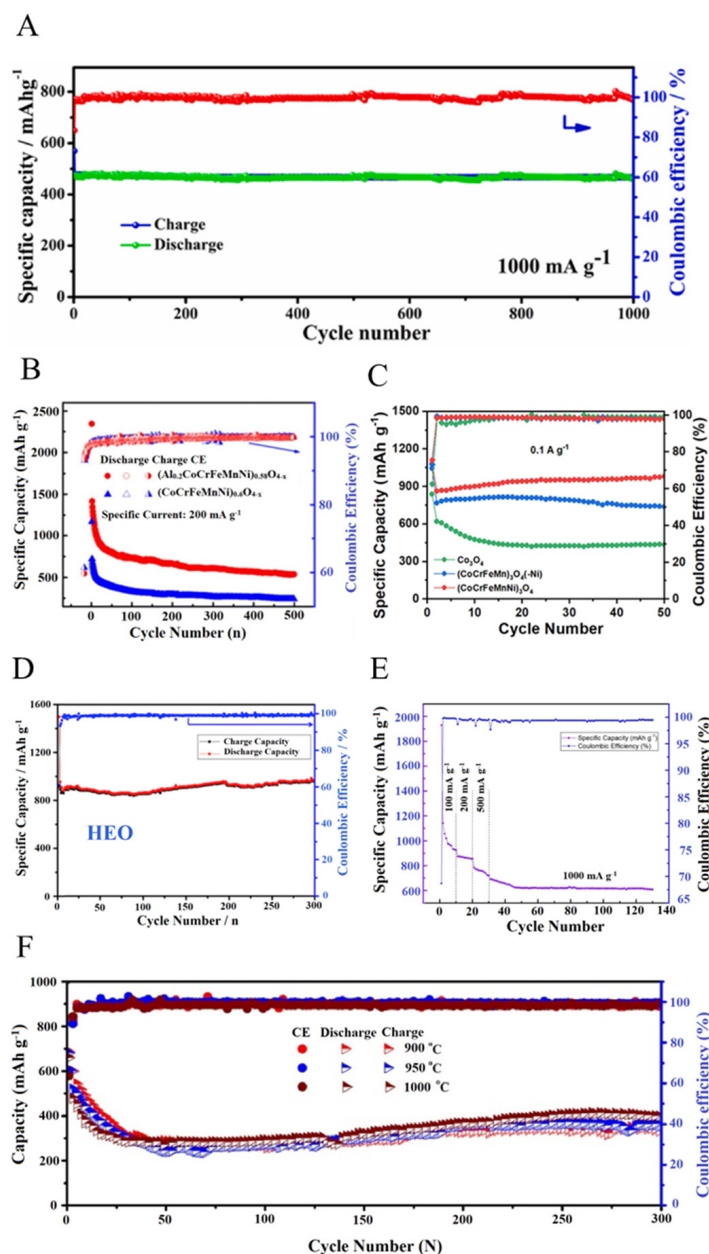


**Figure 4.** Cycle life of high-entropy anodes. (A)  $(\text{Mg}_{0.2}\text{Co}_{0.2}\text{Ni}_{0.2}\text{Cu}_{0.2}\text{Zn}_{0.2})\text{O}$ ; (B)  $(\text{Al}_{0.2}\text{CoCrFeMnNi})_{0.58}\text{O}_{4-x}$ ; (C)  $(\text{Co}_{0.2}\text{Cr}_{0.2}\text{Fe}_{0.2}\text{Mn}_{0.2}\text{Ni}_{0.2})_3\text{O}_4$ ; (D)  $\text{Mg}_{0.2}\text{Co}_{0.2}\text{Ni}_{0.2}\text{Cu}_{0.2}\text{Zn}_{0.2}\text{O}$ ; (E)  $(\text{MgCoNiZn})_{0.65}\text{Li}_{0.35}\text{O}$  (F)  $(\text{FeCoNiCrMn})_3\text{O}_4$ . Reprinted with permission from refs. [20–25]. Copyright© 2022 Elsevier; Copyright© 2022 American Chemical Society (Washington, DC, USA); Copyright© 2019 Elsevier; Copyright© 2020 Elsevier; Copyright© 2021 Springer Nature; Copyright© 2021 American Chemical Society.



**Table 2.** Various high-entropy materials employed as potential battery anodes.

Composition	Cycles	Initial Capacity (mAh g <sup>-1</sup> )	Final Capacity (mAh g <sup>-1</sup> )	Current Density	Ref.
Mg <sub>0.2</sub> Co <sub>0.2</sub> Ni <sub>0.2</sub> Cu <sub>0.2</sub> Zn <sub>0.2</sub> O	300	≈1500	≈935	0.1 A g <sup>-1</sup>	[22]
MgCoNiZnCuO-GO	1000	460	460	1.0 A g <sup>-1</sup>	[20]
(MgCoNiZi) <sub>0.65</sub> Li <sub>0.35</sub> O	100	≈680	610	1.0 A g <sup>-1</sup>	[21]
(FeCoNiCrMn) <sub>3</sub> O <sub>4</sub>	300	≈660	402	0.5 A g <sup>-1</sup>	[23]
(Al <sub>0.2</sub> CoCrFeMnNi) <sub>0.58</sub> O <sub>4-δ</sub>	500	2234	536	0.2 A g <sup>-1</sup>	[24]
(CoCrFeMnNi) <sub>3</sub> O <sub>4</sub>	50	1133	980	0.1 A g <sup>-1</sup>	[25]

Silicon is another potential anode due to its extremely high theoretical capacity of 4212 mAh g<sup>-1</sup>. However, its poor cyclability due to a significant volume expansion (~300%) when alloyed with Li restricts its widespread application. This volume expansion can also lead to the rupture of the solid electrolyte interface (SEI) layer that is formed on the surface of the Si anode, causing it to reform with each cycle, resulting in the consumption of Li ions [4]. To address this issue, Si is combined with other elements to create a high-entropy alloy (HEA) that has the potential to retain a high capacity and stabilized crystal structure and restrict the volume expansion. Alloys of Si<sub>49</sub>Cu<sub>42</sub>Ag<sub>7</sub>Sn<sub>2</sub>, while not high-entropy materials, have shown stable capacities around 1000 mAh g<sup>-1</sup> and provide insight into possible future high-entropy alloy compositions [26]. Several other common elements alloy with lithium, such as Al, Zn, Ga, Ge, Ag, Sn, Sb, and Bi, and could be used to replace current graphite anodes with stable electrochemical performance [27].

Rock-salt-based structures have been the most commonly studied crystal structure for new battery anodes. However, other crystal structures, such as the spinel, may also prove useful as a Li-ion battery anode. The spinel structure offers three-dimensional Li<sup>+</sup> diffusion channels and a random distribution of cations at two Wychoff sites [28]. This increased number of diffusion channels allows for higher ionic conductivities, which can accelerate the reversible redox reaction and result in faster charging times and higher capacities.

Battery degradation in graphite anodes is the result of induced stress during lithiation leading to cracking on the electrode surface. Thus, the high structural stability of HEMs can better withstand the lithium insertion with enhanced cycle stability and energy density compared to conventional graphite anodes.

### 3.2. Cathodes

Over the years, several cathode chemistries have been utilized in LIBs. Conventional cathode materials are typically classified into three categories based on their structure; layered oxides (LCO, NMC), spinel oxides (LMO), and polyanion (LFP) [29,30]. Figure 5 gives a summary of some common cathode chemistries and a potential HEM cathode, highlighting their performances and costs.

The most popular structures for cathode chemistries are layered oxides and polyanion structured materials. Lithium cobalt oxide (LCO) is one of the original cathode materials that are primarily used in consumer electronics. However, it is not practical for EVs due to the structural instability caused by delithiation and its high cost resulting from the significant use of cobalt [31]. Nickel manganese cobalt oxide (NMC), a class of layered oxide cathodes, is extensively researched in lithium-ion systems due to their higher specific capacities compared to polyanion materials like lithium iron phosphate (LFP) [31]. NMC cathodes typically have a capacity of around 200 mAh g<sup>-1</sup>, depending on their composition. Spinel and layered oxides exhibit good electronic conductivities and high energy densities [30]. Layered oxides are preferred over the spinel structure, as the latter is challenging to stabilize using conventional synthesis techniques due to its highly oxidized M<sup>3+</sup>/4<sup>+</sup> states [30]. One common spinel structured cathode composition is LiMn<sub>2</sub>O<sub>4</sub>, but it suffers from Mn dissolution and experiences capacity fade, particularly at elevated temperatures [30].

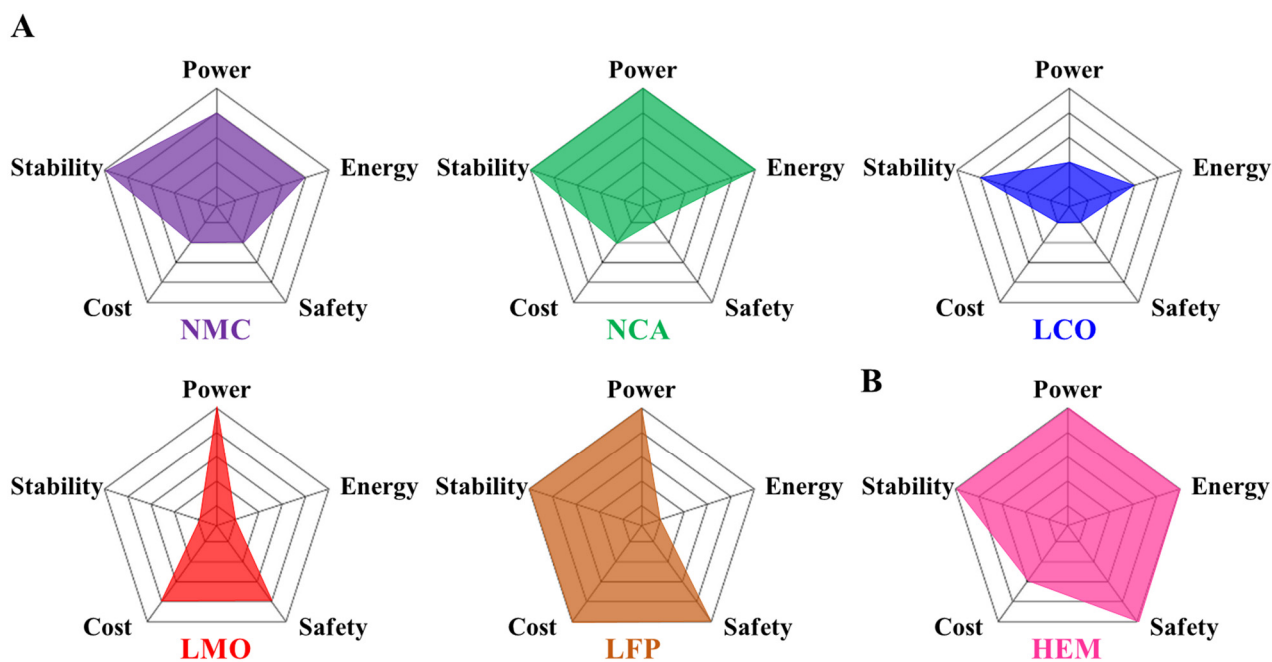


**Figure 5.** Summary of performance metrics of cathodes. (A) Common cathodes. (B) Potential HEM cathode. Reprinted with permission from ref. [31]. Copyright© 2022 MDPI (Basel, Switzerland).

On the other hand, LFP is a polyanion-structured cathode material with a flat discharge plateau and a capacity ranging from 150 to 170 mAh g<sup>-1</sup> [32]. It also offers several advantages over layered oxides, such as high thermal stability, improved safety, and cost-effectiveness. The strong covalent bonding of oxygen to P, S, or Si in the PO<sub>4</sub> tetrahedral unit enables LFP to exhibit a long cycle life and greater electrochemical stability, making it ideal for repeated charging applications [30,31]. Unfortunately, LFP suffers from poor electronic conductivity and often requires additives like conductive carbon, leading to increased manufacturing costs [30]. Due to earth-abundant iron and a long cycle life, LFP may provide better long-term benefits for applications such as EVs and grid energy storage [30,31].

Recent research has shown that high-entropy cathodes can offer a potential replacement for current cathode materials by incorporating various elemental compositions, avoiding toxic or rare elements, and providing increased structural stability through high-entropy stabilization, resulting in improved and unexpected electrochemical performances [33]. HEM cathodes are expected to have fast charging rates, high energy densities, high stability, and high levels of safety. Furthermore, high-entropy materials can now be synthesized relatively easily in both layered oxides and spinel structures, allowing for a wider range of electrochemical performances. Initial attempts at synthesis have been achieved by introducing fluorine and lithium to high-entropy oxide materials. Compositions such as Li<sub>x</sub>(Co<sub>0.2</sub>Mg<sub>0.2</sub>Cu<sub>0.2</sub>Ni<sub>0.2</sub>Zn<sub>0.2</sub>)OF<sub>x</sub> have been synthesized by initially producing the HEO (CoMgCuNiZn)O and ball-milling it with LiF precursors [3,34]. This composition has demonstrated enhanced cycling stability and coulombic efficiency owing to high-entropy stabilization [3,34]. The oxyfluoride transformation has changed the HEO from a conversion-type lithiation mechanism to an insertion-type, thereby increasing the working potential of the material to 3.4 V, compared to an HEO without fluorination of having a potential of 1.0 V [4,35]. Zhao et al. showed that high-entropy materials can be used to stabilize sodium cathode chemistries and were able to maintain a high capacity at charging rates of up to 3 C for 500 cycles, resulting in a capacity retention of 83% [36]. These new types of cathodes provide increased stability, higher site energies for lithium accommodation, and improved energy storage capacity [4]. Table 3 below shows a summary of a select number of high-entropy cathodes and their cycling characteristics. And Figure 6 highlights

the charge and discharge cycling of several different compositions of high-entropy cathodes and show that various compositions of HEMs can extend the cycle life while also increasing the specific capacity of the cathode.

**Table 3.** Various high-entropy materials employed as potential battery cathodes.

Composition	Cycles	Initial Capacity (mAh g <sup>-1</sup> )	Final Capacity (mAh g <sup>-1</sup> )	Rate or Current Density	Ref.
Li <sub>x</sub> (CoCuMgNiZn)OF <sub>x</sub>	300	168	120	C/10	[35]
NaNi <sub>0.12</sub> Cu <sub>0.12</sub> Mg <sub>0.12</sub> Fe <sub>0.15</sub> Co <sub>0.15</sub> Mn <sub>0.1</sub> Ti <sub>0.1</sub> Sn <sub>0.1</sub> Sb <sub>0.04</sub> O <sub>2</sub>	200	110	87	C/2	[36]
Li <sub>0.8</sub> Na <sub>0.2</sub> (NaCoMnAlFe)O <sub>2</sub>	20	80	62	–	[37]
Li(MnCoCrTiNb)OF	20	307	225	20 mA g <sup>-1</sup>	[38]
(CoMgCuNiZn)O	200	1191	664	C/10	[39]

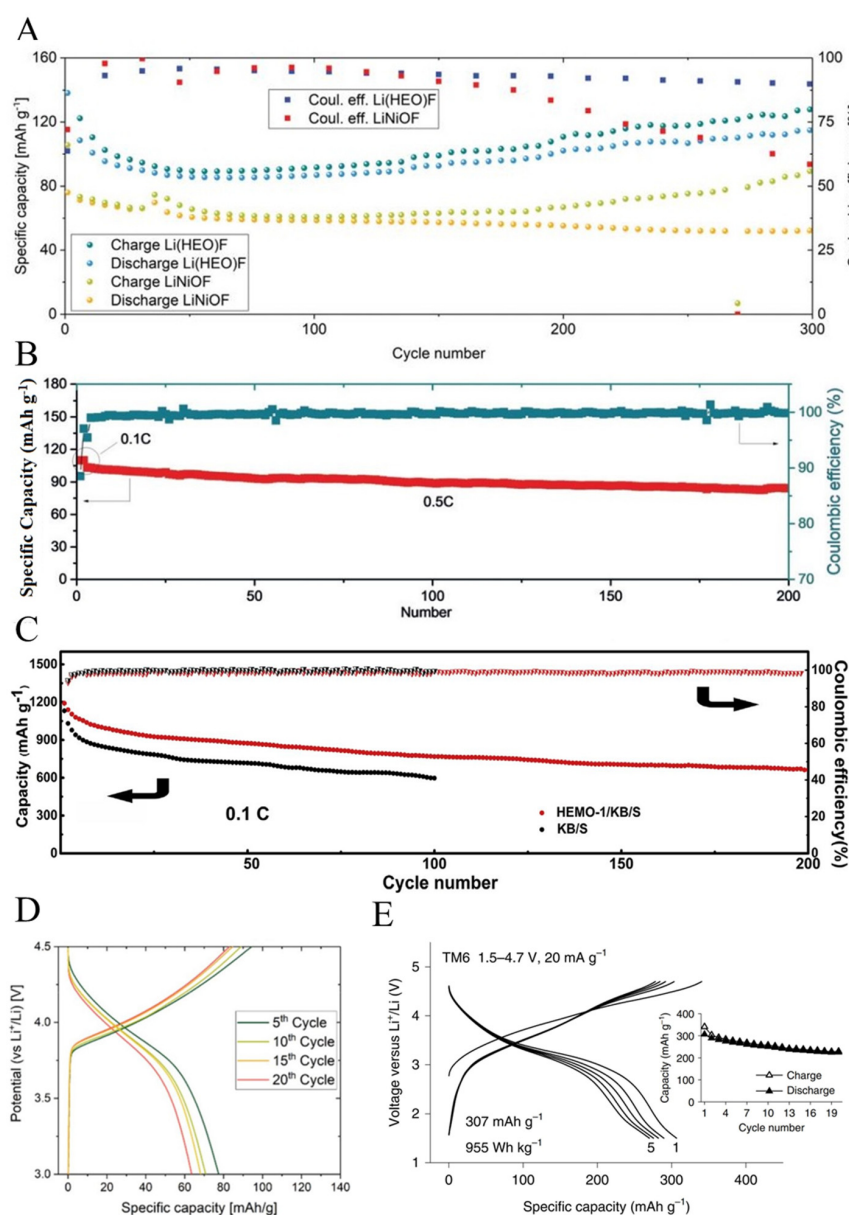


**Figure 6.** Cycling life of high-entropy cathodes. (A) Li<sub>x</sub>(CoCuMgNiZn)OF<sub>x</sub>. Reprinted with permission from ref. [35]. (B) NaNi<sub>0.12</sub>Cu<sub>0.12</sub>Mg<sub>0.12</sub>Fe<sub>0.15</sub>Co<sub>0.15</sub>Mn<sub>0.1</sub>Ti<sub>0.1</sub>Sn<sub>0.1</sub>Sb<sub>0.04</sub>O<sub>2</sub>. Reprinted with permission

from ref. [36]. Copyright© 2020 John Wiley and Sons (Hoboken, NJ, USA). (C) (CoMgCuNiZn)O. Reprinted with permission from ref. [39]. Copyright© 2019 Elsevier. (D)  $\text{Li}_{0.8}\text{Na}_{0.2}(\text{NaCoMnAlFe})\text{O}_2$ . Reprinted with permission from ref. [37]. (E)  $\text{Li}(\text{MnCoCrTiNb})\text{OF}$ . Reprinted with permission from ref. [38]. Copyright© 2020 Spring Nature (Berlin/Heidelberg, Germany).

In addition to new layered and spinel oxide structures for lithium-ion batteries, high-entropy cathodes have also found their application in sodium-ion batteries (NIBs). NIBs have gained much attention in recent times due to their low cost and abundant sodium sources [14]. However, several challenges such as poor structural stability, sluggish ion diffusion, and low operating voltages remain challenges for NIBs [40]. Two commonly employed cathode materials in NIBs are transition metal oxides (TMOs) and polyanionic compounds (PACs). While TMOs have higher theoretical capacities, they often suffer from poor cycling stability of the lattice and low working voltages [41,42]. In contrast, PACs have more structural robustness despite having lower capacities and also exhibit higher working voltages [43]. Cathodes for NIBs are synthesized in a similar way to LIBs. An HEO can be combined with NaF to create a new cathode, such as  $\text{Na}_y(\text{Co}_{0.2}\text{Cu}_{0.2}\text{Mg}_{0.2}\text{Ni}_{0.2}\text{Zn}_{0.2})\text{OCl}$ , which may lead to long-lasting NIBs with better cyclability [2,29]. High-entropy PACs, such as  $\text{Na}_3\text{V}_{1.9}(\text{CaMgAlCrMn})_{0.1}(\text{PO}_4)_2\text{F}_3$ , have demonstrated increased voltage, greater energy density, and superior cycling and provide another avenue for new cathodes [40].

### 3.3. Electrolytes

Lithium-ion batteries are considered the foundation of rechargeable batteries for both portable and electric vehicle applications. Future sodium-ion batteries (NIBs) and current LIBs require electrolytes with high ionic conductivities. Liquid electrolytes have ionic conductivities in the order of  $10^{-3}$ – $10^{-2}$   $\text{S cm}^{-1}$  [44]. However, liquid electrolytes present several issues, such as lithium dendrite growth, the high flammability of the solvents, and thermal hazards [45]. Physical damage and internal electrical damage caused by short circuits can increase the thermal hazards. Additionally, when liquid electrolyte battery packs are made smaller in size through improved manufacturing techniques in an effort to enhance their energy density, the risk of thermal hazards and the possibility of thermal runaway increases. Materials with high  $\text{Li}^+$  and  $\text{Na}^+$  conductivities are crucial for advanced electrolytes to provide long cycling and high reversibility [14]. Therefore, the ideal requirements for future electrolytes include suppression of dendritic growth, enhanced endurance due to changes in the volume of the electrodes during cycling, reduced reactivity of the electrolyte with Li electrodes, improved safety, and improved flexibility and manufacturability [46]. Such an electrolyte should have a high ionic conductivity, electrochemical and interfacial stability, as well as good mechanical strength during cycling and for the ease of manufacturing. The classical electrolytes can be classified into three types: polymer electrolytes, ceramic electrolytes, and liquid electrolytes. Each of these are detailed briefly below.

#### 3.3.1. Polymer Electrolytes

One material that meets several of the requirements for next-generation electrolytes is polymers, with polyethylene oxide (PEO) being the most studied. PEO offers many advantages over other polymers, such as strong electron-donating ether oxygen groups, good thermal stability, and high mechanical toughness [47]. There are three different mechanisms for ion diffusion in solid polymer electrolytes (SPEs): the vacancy mechanism (when an ion moves from its original site to an adjacent vacancy), the interstitial mechanism (when the ions hop from one interstitial site to an adjacent interstitial site), and the knock-out mechanism (where an ion hops to an interstitial site, leaving a vacancy in the original site, where a second ion can then move to the vacant site) [29]. The main challenges with PEO-based SPEs is their high crystallinity at room temperatures, which leads to low ionic conductivity and low salt solubility in the amorphous region at elevated temperatures [46]. Additives have been used as fillers in the PEO matrix to increase the ionic conductivity and reduce crystallinity and to further improve the electrochemical performance. Unary

ceramic additives, such as  $\text{TiO}_2$  and  $\text{Al}_2\text{O}_3$ , both active and inactive, have been employed as additives in SPEs previously, but their doping amount is usually limited to under 20 wt.% due to undesired phases in the polymer causing adverse electrochemical and mechanical properties at higher doping amounts [29,47].

To overcome the limits of unary materials, HEMs have been proposed as fillers for SPEs. High-entropy oxides offer one possibility for SPE additives, as several compositions of HEOs have shown promise, with room-temperature ionic conductivities exceeding  $>10^{-3} \text{ S cm}^{-1}$  [14,29]. Adding highly ionic conductive fillers aims to enhance the underlying conductivity of the polymers and increase their overall electrochemical performance. Ritter et al. demonstrated that through careful selection of elements in a medium-entropy additive, specific properties of the electrolyte, such as a significant increase in the potential voltage window and an enhanced lithium transfer number, could be improved [48]. Therefore, due to their high ionic conductivities and chemically stable structures, high-entropy oxides are excellent candidates for use as fillers in SPE.

### 3.3.2. Ceramic Electrolytes

Ceramic electrolytes have been one of the most studied materials to replace liquid electrolytes in solid-state batteries. High-entropy oxides, such as  $(\text{MgCoNiCuZn})_{1-x-y}\text{Ga}_y\text{A}_x\text{O}$  and  $(\text{MgCoNiCuZn})_{1-x}\text{A}_x\text{O}$  (with A referring to a number of alkali metals such as Li, Na, and K), have shown promise, as they exhibit high ionic conductivities ( $>10^{-3} \text{ S cm}^{-1}$ ) at room temperature [14,29]. The high ionic conductivities are attributed to oxygen vacancies that are created through intrinsic charge compensation when Li, Na, or K is added to the material. The choice of elements and crystal structure significantly influences the final ionic conductivity. While elements such as Co, Ni, Cu, and Zn can actively participate in redox reactions, inactive elements such as Al, Ti, and Mg enhance the chemical stability window [29]. Furthermore, controlling the concentration of the charge-carrying species (Li, Na, or K) is crucial to create fast ion migration channels in the structure. Bérardan et al. were able to synthesis a variety of high-entropy oxides for both  $\text{Li}^+$  and  $\text{Na}^+$  ion conduction, demonstrating large ionic conductivities ( $>10^{-3} \text{ S cm}^{-1}$ ) through the manipulation of oxygen vacancies in the structure [49]. This highlights that the ionic conduction occurs through oxygen vacancies in certain high-entropy oxides. Due to their high ionic conductivities and chemically stable structures, high-entropy oxides are excellent candidates for use as ceramic electrolytes.

### 3.3.3. Liquid Electrolytes

The concept of high entropy has been extended for use in liquid electrolyte systems to enhance overall device performance. One of the popular and commercially used liquid electrolytes is 1.0 M  $\text{LiPF}_6$  salt in a 50:50 blend of EC/DMC solvent. Low temperatures pose challenges for many liquid electrolytes, as their performance deteriorates when the temperature drops. Ethylene carbonate plays a pivotal role in modern electrolyte systems, but when temperatures dip below freezing, a decrease in ionic conductivity due to heightened viscosity is observed, along with precipitate formation on the electrode surface, leading to increased interfacial resistance [50]. For solid HEMs, the entropy of mixing helps stabilize the structure and provides many performance benefits. Similarly, the mixing entropy of the liquid electrolyte can be enhanced by using multiple metal salts and multiple solvents in the electrolyte. In the case of lithium-based electrolytes, an HEM liquid electrolyte involves the use of multiple Li salts that are well dispersed and mixed in the solvent. For example, the ionic conductivity of  $\text{LiPF}_6$  can be further enhanced by additives such as  $\text{LiNO}_3$ ,  $\text{LiFSI}$ ,  $\text{LiTFSI}$ ,  $\text{LiDFOB}$ , and  $\text{LiBETI}$  [51,52]. The use of additional salts results in a wider diversity in the solvation structure and leads to higher lithium-ion mobility [52]. Excess entropy scaling, which is employed to determine the dynamic properties of liquids, such as diffusion constants and heat conductivities, indicates that as the entropy increases, the diffusivity and ionic conductivity increase [52]. This further enhances the overall electrochemical performance and stability. The solvation



structure in liquid electrolytes plays a significant role in charge transfer and solid electrolyte interface (SEI) formation. An interesting side effect caused by the higher solvation structure entropy is a reduction in the electrolyte's melting point, which in turn improves the low-temperature performance [51]. Similar to using multiple Li salts, transitioning from a 50:50 blend of EC:DMC to a mixture of multiple solvents provides additional enhancements [50]. These enhancements include lowering the electrolyte's freezing point and increasing the battery retention and capacity ( $\sim 80 \text{ mAh g}^{-1}$  for decimal solvent vs.  $\sim 8 \text{ mAh g}^{-1}$  for binary solvent). This results in an increase in the ionic conductivity at temperatures as low as  $-60^\circ\text{C}$ , reported to further improve the low-temperature performance of the LIB compared to binary and ternary solvent mixes [50]. The multicomponent basis of HEMs can also be utilized in other battery compositions. For instance, one study demonstrated that adding multiple metal salts (magnesium bis(trifluoromethane sulfonyl)imide ( $\text{Mg}(\text{TFSI})_2$ ) and lithium triflate ( $\text{LiOTf}$ ) and various solvents (1,2-dimethoxyethane (DME) and trimethyl phosphate) to the electrolyte composition improved the interfacial layer in magnesium batteries, resulting in improved electrochemical performance [53]. Figure 7 below depicts the cycling profiles of several distinct high-entropy electrolytes, which encompass ceramics, polymers, and liquid systems. The cycling profiles show that by including HEMs, the long-term cycling stability can be greatly enhanced, resulting in a higher capacity over a larger number of cycles. This increase in long-term cycling is mainly attributed to the structural stability that is provided by the multiple salts and solvents that are now present in the electrolytes.

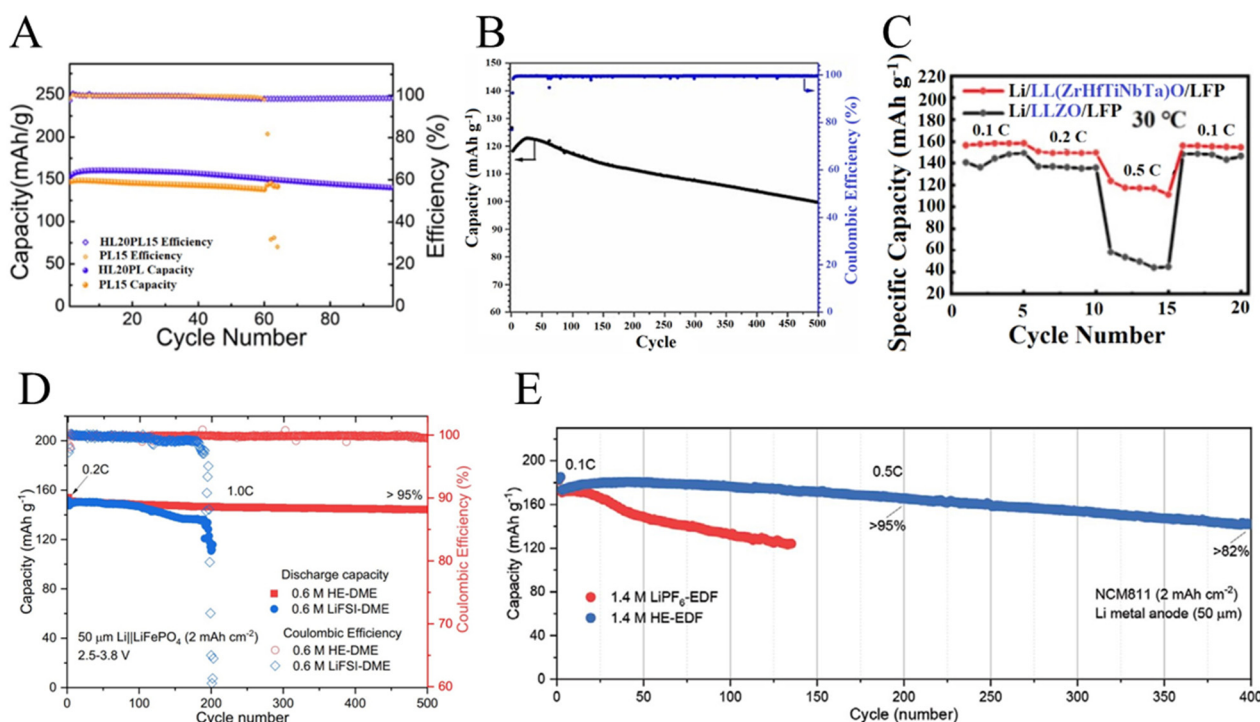


**Figure 7.** Cycling life of high-entropy electrolytes. (A) PEO/LiTFSI/LiMgCoNiCuZn, (B) PEO/LiTFSI/AlTiMgLiO, (C) LL(ZrHfTiNbTa)O, (D) HE-DME (LiFSI, LiTFSI, LiDFOB, LiBETI), (E) HE-EDF (LiFSI, LiTFSI, LiDFOB, LiNO<sub>3</sub>, LiPF<sub>6</sub>). Reprinted with permission from refs. [48,51,54,55]. Copyright© 2022 American Chemical Society. Copyright© 2023 Elsevier.

### 3.4. High-Entropy Materials for Lithium–Sulfur Batteries

High-entropy materials have also been investigated for their potential as separators in lithium–sulfur (Li-S) batteries. Lithium–sulfur batteries are of particular interest due to their cost-effectiveness, sulfur abundance, high theoretical capacity ( $1675 \text{ mAh g}^{-1}$ ), and high energy density ( $2600 \text{ Wh kg}^{-1}$ ), making them promising candidates for next-

generation energy storage systems [14,56]. However, lithium–sulfur batteries have long suffered from capacity fading during cycling, which is primarily attributed to the migration of polysulfides within the electrodes [57,58]. Introducing separators between the sulfur electrodes and the electrolytes aims to reduce the capacity fade in Li-S batteries. One strategy to mitigate the polysulfide migration involves the use of metal oxides in the cathode to physically immobilize and confine the polysulfides [59,60]. Zhou et al. demonstrated that by incorporating MgCrMnFeCoNiO nanoparticles into the sulfur electrode, benefits such as accommodating active species and withstanding volume changes during charge/discharge cycles were achieved [61]. This resulted in a stable capacity of  $1100 \text{ mAh g}^{-1}$  at  $0.5 \text{ C}$  for 1200 cycles [61]. When the HEM material was not included in the sulfur cathode, there was a stark decrease in both capacity ( $312.3 \text{ mAh g}^{-1}$ ) and cycling life (325 cycles) [61]. Raza et al. studied the effects of a sulfur electrode and the addition of cathodes containing a low-entropy oxide, medium-entropy oxide, and high-entropy oxide cathode [62]. The high-entropy additive showed an overall higher initial capacity of  $1233 \text{ mAh g}^{-1}$ , while those of the medium-entropy ( $980 \text{ mAh g}^{-1}$ ) and low-entropy ( $908 \text{ mAh g}^{-1}$ ) additive and sulfur only ( $966 \text{ mAh g}^{-1}$ ) were all reduced [62]. Additionally, the high-entropy additive demonstrated a significantly lower capacity decay rate per cycle ( $\sim 0.043\%$ ) compared to the other cathodes ( $\sim 0.36\%$ ), maintaining a cycle life of 800 cycles at  $0.5 \text{ C}$  [62]. The addition of HEMs increases the long-term cycling stability by confining the movement of polysulfides while also increasing the capacity of the Li-S batteries. High-entropy oxides offer further improvements over binary oxides due to the synergistic immobilization effect that is created by the presence of multiple metal ions [14]. Figure 8 highlights the cycling profiles of high-entropy materials used in Li-S batteries, with a summary of their electrochemical performances being found in Table 4. Not only do HEOs enhance the overall structural stability of the cathode, they also increase the number of active sites that can contain polysulfides, thereby improving the overall battery performance.

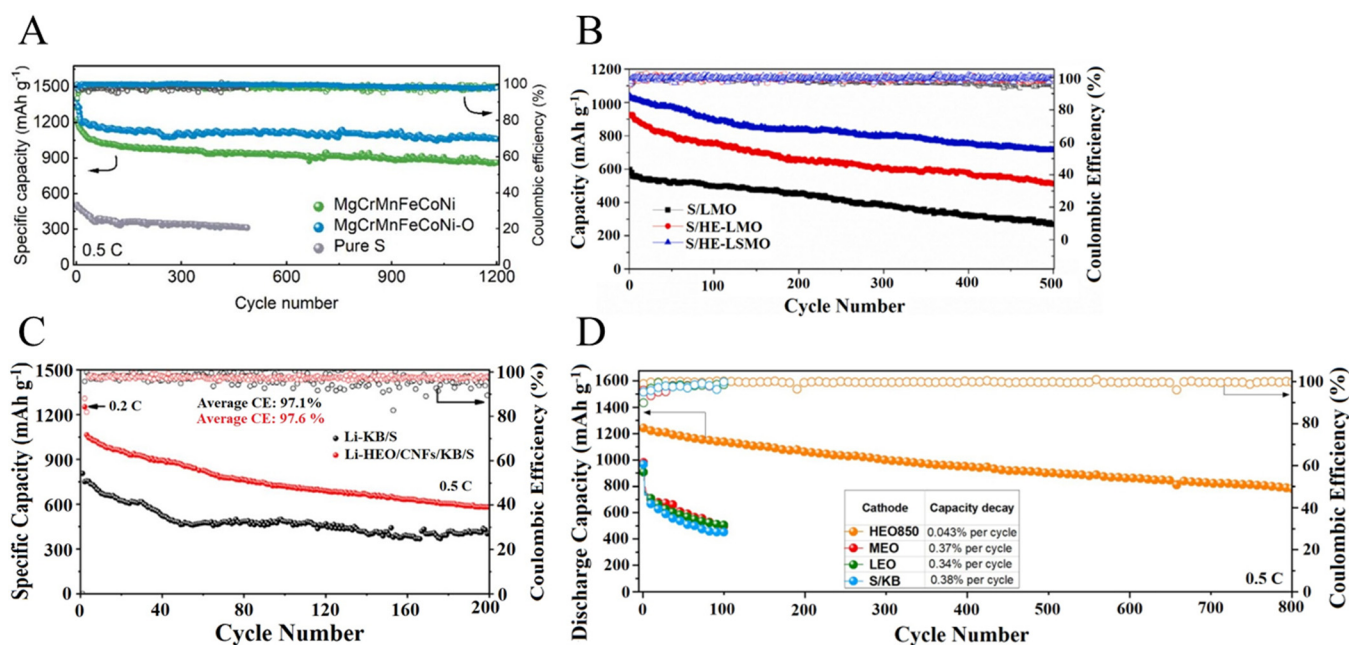


**Figure 8.** Cycling life of high-entropy lithium–sulfur batteries. (A) Cycling performance of MgCrMnFeCoNi cells at a current density of  $0.5 \text{ C}$ . (B) Cycling stability at  $1 \text{ C}$  of S/HE-LSMO, S/HE-LMO and S/LMO composites. (C) Cycling stability of Li-KB/S and Li-HEO/CNFs/KB/S at  $0.5 \text{ C}$ . (D) Comparison of long-term cycling stability of HEO850/S/KB, MEO850/S/KB, LEO850/S/KB, and S/KB cells at  $0.5 \text{ C}$ . Reprinted with permission from refs. [61–64]. Copyright© 2022 Elsevier. Copyright© 2023 John Wiley & Sons Australia, Ltd. (Melbourne, VIC, Australia). Copyright© 2023 Elsevier. Copyright© 2023 Royal Society of Chemistry.

**Table 4.** Various high-entropy materials used in lithium–sulfur batteries.

Composition	Cycles	Initial Capacity (mAh g <sup>-1</sup> )	Final Capacity (mAh g <sup>-1</sup> )	Rate	Sulfur Loading (mg cm <sup>-2</sup> )	Ref.
(MgCrMnFeCoNi)O/Sulfur/ Carbon black/PVDF	1200	1397	1100	0.5 C	4.5	[61]
(Cu <sub>0.7</sub> Ni <sub>0.6</sub> Fe <sub>0.6</sub> Sn <sub>0.5</sub> Mn <sub>0.4</sub> )O <sub>4</sub> /CNF	400	907	435	1 C	1.1	[63]
La <sub>0.8</sub> Sr <sub>0.2</sub> (Cr <sub>0.2</sub> Mn <sub>0.2</sub> Fe <sub>0.2</sub> Co <sub>0.2</sub> Ni <sub>0.2</sub> )O <sub>3</sub> / Sulfur/PVDF/CNF	500	1038	714	1 C	1.3–1.5	[64]
(Ni <sub>0.2</sub> Co <sub>0.2</sub> Cu <sub>0.2</sub> Mg <sub>0.2</sub> Zn <sub>0.2</sub> )O/Sulfur/ Ketjen Black	800	1244	784	0.5 C	1.2	[62]

### 3.5. High-Entropy Catalysts in Metal–Air Batteries

High-entropy materials have been a subject of study for several years in the field of catalysis. Catalysts play a crucial role in various industrial processes, and HEMs have shown promising results in several reactions, including methanol oxidation, ethanol oxidation, oxygen reduction, hydrogen evolution reaction, and water splitting [2,14,65]. In many of these reactions, HEMs can provide increased chemical stability, reduced costs by reduction of precious metals, corrosion resistance, and high temperature stability [2,65]. Metal–air batteries, such as lithium–air and zinc–air batteries, encounter similar cycling issues to Li-S systems, as mentioned above. During cycling, the oxygen evolution reaction can generate byproducts like Zn(OH)<sub>4</sub> for zinc–air batteries and LiOH and Li<sub>2</sub>CO<sub>3</sub> for lithium–air batteries [66,67]. High-entropy materials possess a substantial number of surface active sites that can be utilized to mitigate the formation of unwanted chemical species during the charge/discharge cycles, thereby enhancing the performance of these battery types [66]. These side reactions become more challenging when operating in real-world conditions, using atmospheric air instead of pure O<sub>2</sub>, as atmospheric air contains other components such as H<sub>2</sub>O, CO<sub>2</sub>, and N<sub>2</sub> [67]. Yu et al. demonstrated how the addition of different elements, such as Mo and V, to a base quinary AlNiCoFeCr system improved the oxygen evolution reaction (OER) activity. However, when further elements such as Cu, Nb, or Ti were added and the total number of elements increased, the OER activity began to decrease [68]. Moreover, altering the ratios of Ni, Co, Fe, and Cr resulted in a varied OER performance. Increasing the Ni or Cr concentration had little effect on the OER performance, whereas an increase in the Fe concentration clearly decreased the OER performance [68]. The choice of elements and their atomic ratios in an HEM can significantly impact its final activity and needs to be carefully designed to achieve optimal results. Figure 9 highlights the discharge curves of several metal–air batteries, with a summary of their performance in Table 5, showcasing the overall improvement in energy density when HEMs are used over more traditional Pt. Due to the structural complexity of high-entropy materials, finding a suitable catalyst to improve metal–air batteries' performance remains an ongoing endeavor and a scope for future research.

**Table 5.** Various high-entropy materials used in metal–air batteries.

Composition	Rate (mA cm <sup>-2</sup> )	Open Circuit Voltage (V)	Energy Density (Wh kg <sup>-1</sup> )	Ref.
AlNiCoRuMoCrFeTi	20	1.51	923.7	[69]
PtPdAuAgCuIrRu on AlNiCoFeCrMoTiO	20	1.53	897.6	[70]
AlNiCoFeCrMoV/CoNC	20	1.50	950.0	[68]
PdNiVAuMnIrFeCuCoMoPtRu	20	1.50	952.0	[71]
Pt/C-IrO <sub>2</sub>	20	1.46	812.8	[70]

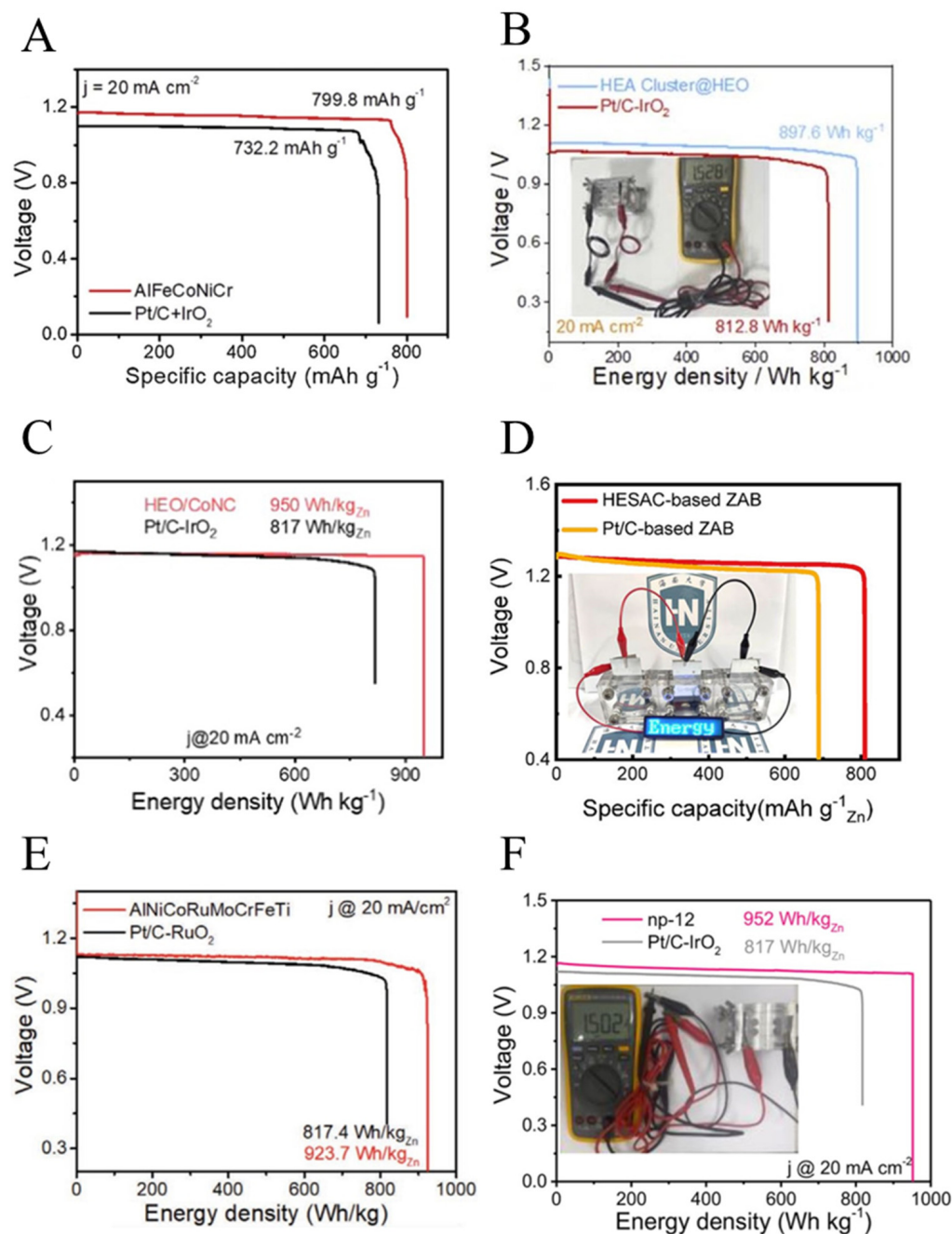


**Figure 9.** Discharge curves of metal–air batteries. (A) AlFeCoNiCr at  $20 \text{ mA cm}^{-2}$ . (B) PtPdAuAgCuIrRu on AlNiCoFeCrMoTiO at  $20 \text{ mA cm}^{-2}$ . (C) AlNiCoFeCrMoV/CoNC at  $20 \text{ mA cm}^{-2}$ . (D) FeCoNiCuMn. (E) AlNiCoRuMoCrFeTi at  $20 \text{ mA cm}^{-2}$ . (F) PdNiVAuMnIrFeCuCoMoPtRu at  $20 \text{ mA cm}^{-2}$ . Reprinted with permission from refs. [68–73]. Copyright© 2020 Elsevier B.V. Copyright© 2022 Wiley-VCH GmbH (Weinheim, Germany). Copyright© 2023 Elsevier. Copyright© 2022 Royal Society of Chemistry. Copyright© 2022 American Chemical Society.

#### 4. Challenges and Perspectives

There is a double-edged sword when it comes to high-entropy materials. On the one hand, there is a vast array of available compositions, with an innumerable number of properties that are yet to be discovered. At the same time, analyzing these various compositions can be an exhaustive task, often resulting in a trial-and-error approach to material design. New approaches may be needed to truly harness the potential of high-entropy materials. As the database of high-entropy materials grows, it could lead

to more computer-based algorithms, such as artificial intelligence (AI), being used to study and predict future possible compositions. Also, an increase in the deployment of Density Functional Theory (DFT)-based methods can result in demand-driven material design. Fundamentally, for HEMs in general, but also as they relate to batteries, there is a need for more tailored design of HEMs for specific needs or properties. This requires a better understanding of how each individual element interacts with other elements in the material. More studies that explore this interaction will go a long way toward tailoring future materials.

Additionally, the scalability of HEM manufacturing still requires further exploration. While several methods have the potential to greatly expand production, such as ball milling, electrochemical, microwave, and aerosol synthesis methods, these methods have mainly been used for small-batch and research studies. For high-entropy materials to make a significant difference in future battery components, production volumes will need to expand by orders of magnitude. Finding an efficient and cost-effective method of large-scale production will be required for further exploitation of high-entropy materials in batteries.

## 5. Conclusions and Future Directions

The ongoing quest for high-energy Li-ion batteries has resulted in incremental changes to current anodes, cathodes, and electrolyte compositions. In cathodes, high-entropy materials can create new layered structures that enhance long-term cycling. High-entropy anodes can offer highly specific capacitance along with a long cycle life, while reducing the dependency on hard-to-mine elements such as lithium and cobalt. HEMs incorporated into electrolytes can lead to improved interfaces, higher ionic conductivities, increased cycling life, and increased stability. High-entropy catalysts can play a role in the migration of polysulfides in Li-S and metal-air batteries, leading to longer cycling with less degradation of the battery. With this scope of various performance improvements, HEMs can be employed in other battery chemistries as well, such as sodium, sulfur, silicon, and lithium-metal batteries, which can further boost energy densities and create safe and long-lasting batteries. The challenge of producing HEMs in sufficient quantities to impact future large-scale applications has been addressed by several researchers, who have developed synthesis techniques that can be scaled to industrial levels. It is now possible to manufacture HEMs with a diverse range of elements and crystal structures and through various high-yield synthesis methods. The key to utilizing these materials in future batteries lies in their seamless integration into current battery manufacturing processes. This integration requires synthesis techniques that consistently yield high-quality HEMs at a low cost, along with the capability to incorporate these materials into existing anodes, cathodes, separators, and electrolytes. There are still several paths of research that need to be explored to fully implement high-entropy materials into energy storage applications:

- (1) More studies are required to understand the underlying mechanisms that result in the performance increases that were observed in the current studies. The increased performance is generally associated with the “cocktail effect” that is linked to all high-entropy materials.
- (2) Additional research is needed to understand how various elements react with each other, and understanding their roles in the system is necessary to better design future HEMs. For instance, the inclusion of Mg plays a role in stabilizing the structure, while other elements such as Ni, Co, and Mn have roles in increased capacity. Studies can incorporate machine learning to better determine possible future compositions based on electrochemical targets such as specific capacity, ionic conductivity, or cycle life. Additional studies are required to better understand how each individual element contributes to the improved electrochemical performance of the system from a fundamental perspective. Studies focusing on bond lengths, angles, and other structural relationships may yield insights into how the structural stability of the HEMs enhances their performance or how differing elements and their bond lengths affect the ionic conductivity.



- (3) Overall efficiency improvements to the various battery components when HEMs are utilized are still needed. Further studies of different crystal structures, especially ones that include multiple Wyckoff sites, are essential due to the availability of several high-entropy crystal structures. A better understanding of factors such as the synthesis technique, particle sizes, and morphology is required to ascertain their role in the electrochemical performance. Now that several synthesis paths are possible for a given composition, the role of these various synthesis paths should be studied to determine if any parameters affect battery performance. Additionally, the inclusion of HEMs as additives in other systems should be examined, as seen in cases like HEMs being used in Li-S cathodes.
- (4) Further consideration needs to be given to the future scalability of HEMs. As these materials gain popularity for various applications, attention must be directed towards determining the optimal approach for scaling this new class of materials to industrial production levels. The synthesis of HEMS should prioritize being cost-effective, rapid, high-quality, and yielding high quantities. This approach will enable the exploitation of their properties in future battery materials.

**Author Contributions:** T.G.R. and R.S.-Y. wrote the paper. S.P. has reviewed and edited the entire text. All authors discussed the results and commented on the manuscript. All authors have read and agreed to the published version of the manuscript.

**Funding:** This research was funded by the National Science Foundation, grant number DMR-2313395.

**Data Availability Statement:** No new data were created or analyzed in this study. Data sharing is not applicable to this article.

**Conflicts of Interest:** The authors declare no conflicts of interest.

## References

1. Li, Q.; Yu, X.; Li, H.; Chen, L. The Road Towards High Energy Density Batteries. *Innov. Energy* **2024**, *1*, 100005. [[CrossRef](#)]
2. Shahbazian-Yassar, R.; Amiri, A. Recent Progress of High Entropy Materials for Energy Storage and Conversion. *J. Mater. Chem. A* **2021**, *9*, 782–823. [[CrossRef](#)]
3. Ma, Y.; Ma, Y.; Wang, Q.; Schweidler, S.; Botros, M.; Fu, T.; Hahn, H.; Brezesinski, T.; Breitung, B. High-Entropy Energy Materials: Challenges and New Opportunities. *Energy Environ. Sci.* **2021**, *14*, 2883–2905. [[CrossRef](#)]
4. Sturman, J.W.; Baranova, E.A.; Abu-Lebdeh, Y. Review: High-Entropy Materials for Lithium-Ion Battery Electrodes. *Front. Energy Res.* **2022**, *10*, 1–15. [[CrossRef](#)]
5. Miracle, D.B.; Senkov, O.N. A Critical Review of High Entropy Alloys and Related Concepts. *Acta Mater.* **2017**, *122*, 448–511. [[CrossRef](#)]
6. Xiang, H.; Xing, Y.; Dai, F.; Wang, H.; Su, L.; Wang, H.; Zhao, B.; Li, J.; Zhou, Y. High-Entropy Ceramics: Present Status, Challenges, and a Look Forward. *J. Adv. Ceram.* **2021**, *10*, 385–441. [[CrossRef](#)]
7. Zhang, Y.; Zuo, T.T.; Tang, Z.; Gao, M.C.; Dahmen, K.A.; Liaw, P.K.; Lu, Z.P. Microstructures and Properties of High-Entropy Alloys. *Prog. Mater. Sci.* **2014**, *61*, 1–93. [[CrossRef](#)]
8. Shojaei, Z.; Khayati, G.R.; Darezereshki, E. Review of Electrodeposition Methods for the Preparation of High-Entropy Alloys. *Int. J. Miner. Metall. Mater.* **2022**, *29*, 1683–1696. [[CrossRef](#)]
9. Zhang, W.; Liaw, P.K.; Zhang, Y. Science and Technology in High-Entropy Alloys. *Sci. China Mater.* **2018**, *61*, 2–22. [[CrossRef](#)]
10. Ritter, T.G.; Phakatkar, A.H.; Rasul, M.G.; Saray, M.T.; Sorokina, L.V.; Shokuhfar, T.; Gonçalves, J.M.; Shahbazian-Yassar, R. Electrochemical Synthesis of High Entropy Hydroxides and Oxides Boosted by Hydrogen Evolution Reaction. *Cell Rep. Phys. Sci.* **2022**, *3*, 100847. [[CrossRef](#)]
11. Phakatkar, A.H.; Saray, M.T.; Rasul, G.; Sorokina, L.V.; Ritter, T.; Shokuhfar, T.; Shahbazian-yassar, R. Ultrafast Synthesis of High Entropy Oxide Nanoparticles by Flame Spray Pyrolysis. *Langmuir* **2021**, *37*, 9059–9068. [[CrossRef](#)] [[PubMed](#)]
12. Dąbrowa, J.; Stygar, M.; Mikuła, A.; Knapik, A.; Mroczka, K.; Tejchman, W.; Danielewski, M.; Martin, M. Synthesis and Microstructure of the (Co,Cr,Fe,Mn,Ni)<sub>3</sub>O<sub>4</sub> High Entropy Oxide Characterized by Spinel Structure. *Mater. Lett.* **2018**, *216*, 32–36. [[CrossRef](#)]
13. Xiang, H.; Dai, F.-Z.; Zhou, Y. *High Entropy Materials from Basics to Applications*; Wiley-VCH: Weinheim, Germany, 2023.
14. Akrami, S.; Edalati, P.; Fuji, M.; Edalati, K. High-Entropy Ceramics: Review of Principles, Production and Applications. *Mater. Sci. Eng. R Rep.* **2021**, *146*, 100644. [[CrossRef](#)]
15. Fang, S.; Bresser, D.; Passerini, S. Transition Metal Oxide Anodes for Electrochemical Energy Storage in Lithium- and Sodium-Ion Batteries. *Adv. Energy Mater.* **2020**, *10*, 1902485. [[CrossRef](#)]

16. Wu, W.; Wang, M.; Wang, J.; Wei, Z.; Zhang, T.; Chi, S.-S.; Wang, C.; Deng, Y. Transition Metal Oxides as Lithium-Free Cathodes for Solid-State Lithium Metal Batteries. *Nano Energy* **2020**, *74*, 104867. [[CrossRef](#)]
17. Sarkar, A.; Velasco, L.; Wang, D.; Wang, Q.; Talasila, G.; de Biasi, L.; Kübel, C.; Brezesinski, T.; Bhattacharya, S.S.; Hahn, H.; et al. High Entropy Oxides for Reversible Energy Storage. *Nat. Commun.* **2018**, *9*, 3400. [[CrossRef](#)] [[PubMed](#)]
18. Ortiz, M.G.; Visintin, A.; Real, S.G. Synthesis and Electrochemical Properties of Nickel Oxide as Anodes for Lithium-Ion Batteries. *J. Electroanal. Chem.* **2021**, *883*, 114875. [[CrossRef](#)]
19. Wang, L.; Zhang, G.; Liu, Q.; Duan, H. Recent Progress in Zn-Based Anodes for Advanced Lithium Ion Batteries. *Mater. Chem. Front.* **2018**, *2*, 1414–1435. [[CrossRef](#)]
20. Guo, H.; Shen, J.; Wang, T.; Cheng, C.; Yao, H.; Han, X.; Zheng, Q. Design and Fabrication of High-Entropy Oxide Anchored on Graphene for Boosting Kinetic Performance and Energy Storage. *Ceram. Int.* **2022**, *48*, 3344–3350. [[CrossRef](#)]
21. Lökçü, E.; Toparli, Ç.; Anik, M. Electrochemical Performance of  $(\text{MgCoNiZn})_{1-x}\text{Li}_x\text{O}$  High-Entropy Oxides in Lithium-Ion Batteries. *ACS Appl. Mater. Interfaces* **2020**, *12*, 23860–23866. [[CrossRef](#)]
22. Qiu, N.; Chen, H.; Yang, Z.; Sun, S.; Wang, Y.; Cui, Y. A High Entropy Oxide  $(\text{Mg}_{0.2}\text{Co}_{0.2}\text{Ni}_{0.2}\text{Cu}_{0.2}\text{Zn}_{0.2}\text{O})$  with Superior Lithium Storage Performance. *J. Alloys Compd.* **2019**, *777*, 767–774. [[CrossRef](#)]
23. Wang, D.; Jiang, S.; Duan, C.; Mao, J.; Dong, Y.; Dong, K.; Wang, Z.; Luo, S.; Liu, Y.; Qi, X. Spinel-Structured High Entropy Oxide  $(\text{FeCoNiCrMn})_3\text{O}_4$  as Anode Towards Superior Lithium Storage Performance. *J. Alloys Compd.* **2020**, *844*, 156158. [[CrossRef](#)]
24. Xiang, H.Z.; Xie, H.X.; Chen, Y.X.; Zhang, H.; Mao, A.; Zheng, C.H. Porous Spinel-Type  $(\text{Al}_{0.2}\text{CoCrFeMnNi})_{0.58}\text{O}_{4-\delta}$  High-Entropy Oxide as a Novel High-Performance Anode Material for Lithium-Ion Batteries. *J. Mater. Sci.* **2021**, *56*, 8127–8142. [[CrossRef](#)]
25. Zhao, J.; Yang, X.; Huang, Y.; Du, F.; Zeng, Y. Entropy Stabilization Effect and Oxygen Vacancies Enabling Spinel Oxide Highly Reversible Lithium-Ion Storage. *ACS Appl. Mater. Interfaces* **2021**, *13*, 58674–58681. [[CrossRef](#)] [[PubMed](#)]
26. Dahn, J.R.; Mar, R.E.; Fleischauer, M.D.; Obrovac, M.N. The Impact of the Addition of Rare Earth Elements to  $\text{Si}_{1-x}\text{Sn}_x$  Negative Electrode Materials for Li-Ion Batteries. *J. Electrochem. Soc.* **2006**, *153*, A1211. [[CrossRef](#)]
27. Obrovac, M.N.; Chevrier, V.L. Alloy Negative Electrodes for Li-Ion Batteries. *Chem. Rev.* **2014**, *114*, 11444–11502. [[CrossRef](#)] [[PubMed](#)]
28. Liu, X. High-Entropy Oxide: A Future Anode Contender for Lithium-Ion Battery. *EcoMat* **2022**, *4*, e12261. [[CrossRef](#)]
29. Chen, Y.; Fu, H.; Huang, Y.; Huang, L.; Zheng, X.; Dai, Y.; Huang, Y.; Luo, W. Opportunities for High-Entropy Materials in Rechargeable Batteries. *ACS Mater. Lett.* **2021**, *3*, 160–170. [[CrossRef](#)]
30. Manthiram, A. A Reflection on Lithium-Ion Battery Cathode Chemistry. *Nat. Commun.* **2020**, *11*, 1–9. [[CrossRef](#)]
31. Houache, M.S.E.; Yim, C.H.; Karkar, Z.; Abu-Lebdeh, Y. On the Current and Future Outlook of Battery Chemistries for Electric Vehicles—Mini Review. *Batteries* **2022**, *8*, 70. [[CrossRef](#)]
32. Mekonnen, Y.; Sundararajan, A.; Sarwat, A.I. A Review of Cathode and Anode Materials for Lithium-Ion Batteries. In Proceedings of the SoutheastCon 2016, Norfolk, VA, USA, 30 March–3 April 2016; pp. 1–6. [[CrossRef](#)]
33. Lin, Y.; Luo, N.; Chamas, M.; Hu, C.; Grasso, S. Sustainable High-Entropy Ceramics for Reversible Energy Storage: A Short Review. *Int. J. Appl. Ceram. Technol.* **2021**, *18*, 1560–1569. [[CrossRef](#)]
34. Oses, C.; Toher, C.; Curtarolo, S. High-Entropy Ceramics. *Nat. Rev. Mater.* **2020**, *5*, 295–309. [[CrossRef](#)]
35. Wang, Q.; Sarkar, A.; Wang, D.; Velasco, L.; Azmi, R.; Bhattacharya, S.S.; Bergfeldt, T.; Düvel, A.; Heitjans, P.; Brezesinski, T.; et al. Multi-Anionic and -Cationic Compounds: New High Entropy Materials for Advanced Li-Ion Batteries. *Energy Environ. Sci.* **2019**, *12*, 2433–2442. [[CrossRef](#)]
36. Zhao, C.; Ding, F.; Lu, Y.; Chen, L.; Hu, Y.S. High-Entropy Layered Oxide Cathodes for Sodium-Ion Batteries. *Angew. Chemie-Int. Ed.* **2020**, *59*, 264–269. [[CrossRef](#)] [[PubMed](#)]
37. Wang, J.; Cui, Y.; Wang, Q.; Wang, K.; Huang, X.; Stenzel, D.; Sarkar, A.; Azmi, R.; Bergfeldt, T.; Bhattacharya, S.S.; et al. Lithium Containing Layered High Entropy Oxide Structures. *Sci. Rep.* **2020**, *10*, 1–13. [[CrossRef](#)] [[PubMed](#)]
38. Lun, Z.; Ouyang, B.; Kwon, D.H.; Ha, Y.; Foley, E.E.; Huang, T.Y.; Cai, Z.; Kim, H.; Balasubramanian, M.; Sun, Y.; et al. Cation-Disordered Rocksalt-Type High-Entropy Cathodes for Li-Ion Batteries. *Nat. Mater.* **2021**, *20*, 214–221. [[CrossRef](#)] [[PubMed](#)]
39. Zheng, Y.; Yi, Y.; Fan, M.; Liu, H.; Li, X.; Zhang, R.; Li, M.; Qiao, Z.A. A High-Entropy Metal Oxide as Chemical Anchor of Polysulfide for Lithium-Sulfur Batteries. *Energy Storage Mater.* **2019**, *23*, 678–683. [[CrossRef](#)]
40. Gu, Z.Y.; Guo, J.Z.; Cao, J.M.; Wang, X.T.; Zhao, X.X.; Zheng, X.Y.; Li, W.H.; Sun, Z.H.; Liang, H.J.; Wu, X.L. An Advanced High-Entropy Fluorophosphate Cathode for Sodium-Ion Batteries with Increased Working Voltage and Energy Density. *Adv. Mater.* **2022**, *34*, 1–10. [[CrossRef](#)]
41. Zuo, W.; Qiu, J.; Liu, X.; Ren, F.; Liu, H.; He, H.; Luo, C.; Li, J.; Ortiz, G.F.; Duan, H.; et al. The Stability of P2-Layered Sodium Transition Metal Oxides in Ambient Atmospheres. *Nat. Commun.* **2020**, *11*, 1–12. [[CrossRef](#)]
42. Xiao, Y.; Zhu, Y.F.; Yao, H.R.; Wang, P.F.; Zhang, X.D.; Li, H.; Yang, X.; Gu, L.; Li, Y.C.; Wang, T.; et al. A Stable Layered Oxide Cathode Material for High-Performance Sodium-Ion Battery. *Adv. Energy Mater.* **2019**, *9*, 1–8. [[CrossRef](#)]
43. Jin, T.; Li, H.; Zhu, K.; Wang, P.F.; Liu, P.; Jiao, L. Polyanion-Type Cathode Materials for Sodium-Ion Batteries. *Chem. Soc. Rev.* **2020**, *49*, 2342–2377. [[CrossRef](#)] [[PubMed](#)]
44. Yang, H.; Wu, N. Ionic Conductivity and Ion Transport Mechanisms of Solid-State Lithium-Ion Battery Electrolytes: A Review. *Energy Sci. Eng.* **2022**, *10*, 1643–1671. [[CrossRef](#)]
45. Pigłowska, M.; Kurc, B.; Galiński, M.; Fuć, P.; Kamińska, M.; Szymlet, N.; Daszkiewicz, P. Challenges for Safe Electrolytes Applied in Lithium-Ion Cells—A Review. *Materials* **2021**, *14*, 6783. [[CrossRef](#)] [[PubMed](#)]

46. Song, J.Y.; Wang, Y.Y.; Wan, C.C. Review of Gel-Type Polymer Electrolytes for Lithium-Ion Batteries. *J. Power Sources* **1999**, *77*, 183–197. [[CrossRef](#)]
47. Feng, J.; Wang, L.; Chen, Y.; Wang, P.; Zhang, H.; He, X. PEO Based Polymer-Ceramic Hybrid Solid Electrolytes: A Review. *Nano Converg.* **2021**, *8*, 2. [[CrossRef](#)] [[PubMed](#)]
48. Ritter, T.G.; Gonçalves, M.; Stoyanov, S.; Ghorbani, A. AlTiMgLiO Medium Entropy Oxide Additive for PEO-Based Solid Polymer Electrolytes in Lithium Ion Batteries. *J. Energy Storage* **2023**, *72*, 108491. [[CrossRef](#)]
49. Bérardan, D.; Franger, S.; Meena, A.K.; Dragoe, N. Room Temperature Lithium Superionic Conductivity in High Entropy Oxides. *J. Mater. Chem. A* **2016**, *4*, 9536–9541. [[CrossRef](#)]
50. Zhang, W.; Xia, H.; Zhu, Z.; Lv, Z.; Cao, S.; Wei, J.; Luo, Y.; Xiao, Y.; Liu, L.; Chen, X. Decimal Solvent-Based High-Entropy Electrolyte Enabling the Extended Survival Temperature of Lithium-Ion Batteries to  $-130$  °C. *CCS Chem.* **2021**, *3*, 1245–1255. [[CrossRef](#)]
51. Wang, Q.; Zhao, C.; Yao, Z.; Wang, J.; Wu, F.; Kumar, S.G.H.; Ganapathy, S.; Eustace, S.; Bai, X.; Li, B.; et al. Entropy-Driven Liquid Electrolytes for Lithium Batteries. *Adv. Mater.* **2023**, *35*, e2210677. [[CrossRef](#)]
52. Wang, Q.; Zhao, C.; Wang, J.; Yao, Z.; Wang, S.; Kumar, S.G.H.; Ganapathy, S.; Eustace, S.; Bai, X.; Li, B.; et al. High Entropy Liquid Electrolytes for Lithium Batteries. *Nat. Commun.* **2023**, *14*, 440. [[CrossRef](#)]
53. Wang, S.; Wang, K.; Zhang, Y.; Jie, Y.; Li, X.; Pan, Y.; Gao, X.; Nian, Q.; Cao, R.; Li, Q.; et al. High-Entropy Electrolyte Enables High Reversibility and Long Lifespan for Magnesium Metal Anodes. *Angew. Chemie-Int. Ed.* **2023**, *62*, e202304411. [[CrossRef](#)] [[PubMed](#)]
54. Cai, Z.P.; Ma, C.; Kong, X.Y.; Wu, X.Y.; Wang, K.X.; Chen, J.S. High-Performance PEO-Based All-Solid-State Battery Achieved by Li-Conducting High Entropy Oxides. *ACS Appl. Mater. Interfaces* **2022**, *14*, 57047–57054. [[CrossRef](#)] [[PubMed](#)]
55. Han, S.; Wang, Z.; Ma, Y.; Miao, Y.; Wang, X.; Wang, Y.; Wang, Y. Fast Ion-Conducting High-Entropy Garnet Solid-State Electrolytes with Excellent Air Stability. *J. Adv. Ceram.* **2023**, *12*, 1201–1213. [[CrossRef](#)]
56. Goncalves, J.; Santos, E.A.; Martins, P.R.; Silva, C.; Zanin, H. Emerging Medium- and High-Entropy Materials as Catalysts for Lithium-Sulfur Batteries. *Energy Storage Mater.* **2023**, *63*, 102999. [[CrossRef](#)]
57. Huang, J.Q.; Zhang, Q.; Wei, F. Multi-Functional Separator/Interlayer System for High-Stable Lithium-Sulfur Batteries: Progress and Prospects. *Energy Storage Mater.* **2015**, *1*, 127–145. [[CrossRef](#)]
58. Zheng, D.; Wang, G.; Liu, D.; Si, J.; Ding, T.; Qu, D.; Yang, X.; Qu, D. The Progress of Li-S Batteries—Understanding of the Sulfur Redox Mechanism: Dissolved Polysulfide Ions in the Electrolytes. *Adv. Mater. Technol.* **2018**, *3*, 1700233. [[CrossRef](#)]
59. Carter, R.; Oakes, L.; Muralidharan, N.; Cohn, A.P.; Douglas, A.; Pint, C.L. Polysulfide Anchoring Mechanism Revealed by Atomic Layer Deposition of  $V_2O_5$  and Sulfur-Filled Carbon Nanotubes for Lithium-Sulfur Batteries. *ACS Appl. Mater. Interfaces* **2017**, *9*, 7185–7192. [[CrossRef](#)]
60. Sun, Q.; Xi, B.; Li, J.Y.; Mao, H.; Ma, X.; Liang, J.; Feng, J.; Xiong, S. Nitrogen-Doped Graphene-Supported Mixed Transition-Metal Oxide Porous Particles to Confine Polysulfides for Lithium-Sulfur Batteries. *Adv. Energy Mater.* **2018**, *8*, 1–10. [[CrossRef](#)]
61. Zhou, Z.; Chen, Z.; Lv, H.; Zhao, Y.; Wei, H.; Huai, G.; Xu, R.; Wang, Y. High-Entropy Nanoparticle Constructed Porous Honeycomb as a 3D Sulfur Host for Lithium Polysulfide Adsorption and Catalytic Conversion in Li-S Batteries. *J. Mater. Chem. A* **2023**, *11*, 5883–5894. [[CrossRef](#)]
62. Raza, H.; Cheng, J.; Lin, C.; Majumder, S.; Zheng, G.; Chen, G. High-Entropy Stabilized Oxides Derived via a Low-Temperature Template Route for High-Performance Lithium-Sulfur Batteries. *EcoMat* **2023**, *5*, 1–15. [[CrossRef](#)]
63. Fan, H.; Si, Y.; Zhang, Y.; Zhu, F.; Wang, X.; Fu, Y. Grapevine-like High Entropy Oxide Composites Boost High-Performance Lithium Sulfur Batteries as Bifunctional Interlayers. *Green Energy Environ.* **2022**, *9*, 565–572. [[CrossRef](#)]
64. Tian, L.; Zhang, Z.; Liu, S.; Li, G.; Gao, X. High-Entropy Perovskite Oxide Nanofibers as Efficient Bidirectional Electrocatalyst of Liquid-Solid Conversion Processes in Lithium-Sulfur Batteries. *Nano Energy* **2023**, *106*, 108037. [[CrossRef](#)]
65. Knorpp, A.J.; Bell, J.G.; Huangfu, S.; Stuer, M. From Synthesis to Microstructure: Engineering the High-Entropy Ceramic Materials of the Future. *Chimia* **2022**, *76*, 212–222. [[CrossRef](#)] [[PubMed](#)]
66. Haruna, A.B.; Onoh, E.U.; Ozoemena, K.I. Emerging High-Entropy Materials as Electrocatalysts for Rechargeable Zinc-Air Batteries. *Curr. Opin. Electrochem.* **2023**, *39*, 101264. [[CrossRef](#)]
67. Kang, J.H.; Lee, J.; Jung, J.W.; Park, J.; Jang, T.; Kim, H.S.; Nam, J.S.; Lim, H.; Yoon, K.R.; Ryu, W.H.; et al. Lithium-Air Batteries: Air-Breathing Challenges and Perspective. *ACS Nano* **2020**, *14*, 14549–14578. [[CrossRef](#)] [[PubMed](#)]
68. Yu, T.; Xu, H.; Jin, Z.; Zhang, Y.; Qiu, H.J. Noble Metal-Free High-Entropy Oxide/Co-N-C Bifunctional Electrocatalyst Enables Highly Reversible and Durable Zn-Air Batteries. *Appl. Surf. Sci.* **2023**, *610*, 155624. [[CrossRef](#)]
69. Jin, Z.; Lyu, J.; Hu, K.; Chen, Z.; Xie, G.; Liu, X.; Lin, X.; Qiu, H.J. Eight-Component Nanoporous High-Entropy Oxides with Low Ru Contents as High-Performance Bifunctional Catalysts in Zn-Air Batteries. *Small* **2022**, *18*, 1–9. [[CrossRef](#)]
70. Jin, Z.; Zhou, X.; Hu, Y.; Tang, X.; Hu, K.; Reddy, K.M.; Lin, X.; Qiu, H.J. A Fourteen-Component High-Entropy Alloy@oxide Bifunctional Electrocatalyst with a Record-Low  $\Delta E$  of 0.61 V for Highly Reversible Zn-Air Batteries. *Chem. Sci.* **2022**, *13*, 12056–12064. [[CrossRef](#)]
71. Yu, T.; Zhang, Y.; Hu, Y.; Hu, K.; Lin, X.; Xie, G.; Liu, X.; Reddy, K.M.; Ito, Y.; Qiu, H.J. Twelve-Component Free-Standing Nanoporous High-Entropy Alloys for Multifunctional Electrocatalysis. *ACS Mater. Lett.* **2022**, *4*, 181–189. [[CrossRef](#)]

72. Fang, G.; Gao, J.; Lv, J.; Jia, H.; Li, H.; Liu, W.; Xie, G.; Chen, Z.; Huang, Y.; Yuan, Q.; et al. Multi-Component Nanoporous Alloy/(Oxy)Hydroxide for Bifunctional Oxygen Electrocatalysis and Rechargeable Zn-Air Batteries. *Appl. Catal. B Environ.* **2020**, *268*, 118431. [[CrossRef](#)]
73. Rao, P.; Deng, Y.; Fan, W.; Luo, J.; Deng, P.; Li, J.; Shen, Y.; Tian, X. Movable Type Printing Method to Synthesize High-Entropy Single-Atom Catalysts. *Nat. Commun.* **2022**, *13*, 5071. [[CrossRef](#)]

**Disclaimer/Publisher's Note:** The statements, opinions and data contained in all publications are solely those of the individual author(s) and contributor(s) and not of MDPI and/or the editor(s). MDPI and/or the editor(s) disclaim responsibility for any injury to people or property resulting from any ideas, methods, instructions or products referred to in the content.